Journal of Bionic Engineering (2024) 21:2893–2912
https://doi.org/10.1007/s42235-024-00601-8

RESEARCH ARTICLE

Design of BalanSENS: Functional Evaluation in Ankle Preparation Phase

Tugce Ersoy[1] · Elif Hocaoglu[3,4] · Pınar Kaya[2] · Ramazan Unal[1]

Received: 30 June 2024 / Revised: 29 September 2024 / Accepted: 16 October 2024 / Published online: 12 November 2024

Abstract
In this study, we present the design and development evaluation of BalanSENS toward the realization of the Integrated Balance Rehabilitation (I-BaR) framework. BalanSENS is designed to encourage active participation by integrating multi-sensory information with the co-improvement of sensory and motor functions. Moreover, it can offer individual rehabilitation design with the integration of three phases. The first phase provides foot-ankle muscle activation and movement sensation development. In the second phase, sensory weighting skills and upper extremities independence can be improved by using multi-sensory input. In the last/stepping phase, walking parameters are aimed to be improved with modulated distance. The parallel manipulator is designed through simulations to determine actuation properties and analyze the load-bearing capacity and feasibility of the materials. Drawing from simulation outcomes, an operational 3 DoF platform is constructed to demonstrate their design suitability for the I-BaR framework. Furthermore, design evaluations demonstrated promising results in quantifying force and real-time data monitoring during the passive ankle preparation phase.

Keywords Integrated balance rehabilitation (I-BaR) · Robotic rehabilitation · Multi-modal sensory feedback · Postural adjustment

1 Introduction

Neurological disorders are the most common disability and the second most common cause of death worldwide [1]. These disorders are associated with affected Central and Peripheral Nervous Systems (CNS and PNS). The nervous systems integrate information from the visual, vestibular, proprioceptive, and cognitive signals in order to maintain continuous sensory re-weighting and postural control during Activities of Daily Living (ADL) [2]. Disorder in integrating multi-sensory information causes them to experience a lack of balance and motor control, significantly influencing Quality of Life (QoL) [3].

The CNS uses two fundamental muscular adjustments to maintain balance during different conditions, namely, Anticipatory and Compensatory Postural Adjustments (APAs and CPAs). APAs engage and activate the muscles before an impending external/internal perturbation occurs. It reduces the risk of deterioration in balance by regulating the position of the Center of Mass (CoM). CPAs allow the CoM to be re-positioned by controlling the muscles after posture has been disturbed [4–6]. Research shows that falls often occur during daily activities due to postural deficiencies

✉ Tugce Ersoy
tugce.ersoy@ozu.edu.tr

Elif Hocaoglu
ehocaoglu@medipol.edu.tr

Pınar Kaya
pkaya@medipol.edu.tr

Ramazan Unal
ramazan.unal@ozyegin.edu.tr

[1] Mechanical Engineering, Ozyegin University, Orman, 34794 Istanbul, Turkey

[2] Physiotherapy and Rehabilitation, Istanbul Medipol University, Ekinciler, 34810 Istanbul, Turkey

[3] Electrical and Electronics Engineering, Istanbul Medipol University, Ekinciler, 34810 Istanbul, Turkey

[4] SABITA (Research Institute for Health Sciences and Technologies), Istanbul Medipol University, Ekinciler, 34810 Istanbul, Turkey

([7–9]). Furthermore, impairments in APAs or CPAs can negatively affect each other, highlighting the importance of assessing and training both in rehabilitation ([10–12]). Several research results show that rehabilitation programs can improve these adjustments to enhance patients' postural control and decrease fall rate [4, 5]. These studies indicate that exposure to predicted perturbations enhances compensatory muscle activity and body pressure center adjustments, demonstrating that retraining APAs is possible [5].

One method to improve the postural adjustments and decrease the fall rate is through Perturbation-based Balance Training (PBT) [5]. This training aims to perform body movements and improve CoM deviation control by applying large and destructive forces. PBT programs are essential for training balance reactions adaptable to various situations, aspects, amplitudes, and cognitive activities [13]. As balance reactions improve, the ability to respond to unexpected balance loss in daily activities increases, leading to fewer falls [14–16]. While traditional PBT studies used manual pushes and pulls by physiotherapists, recent methods include treadmill acceleration-deceleration and moving platforms to simulate real-life perturbations [17, 18]. Perturbation training while walking is suggested as effective in reducing falls among the elderly, with improvements in balance control lasting up to a year [5]. Some studies even indicate that a single PBT session can lead to lasting improvements in reactive balance [19–21].

Some of the PBT applications with robot-assisted rehabilitation are studies on balance platforms. The robotic balance platforms aim to improve patients' postural adjustments depending on the position of the CoM and Electromyography (EMG) [22]. Various platforms have been commercialized, e.g., Hunovo [23], Bobo Balance [24], gePRO [25], and Huber 360 [26]. These Degrees of Freedom (DoF) systems intentionally imbalance patients. However, due to the lack of sensory stimulation, weight transfer training for balance cannot be provided. Also, there are platforms in balance rehabilitation, such as MRABT, targeted at post-stroke patients. It supports the patient at the hip with a parallel robotic arm mounted on a movable platform. When the patient's CoM deviates from the predetermined safe area, the compliant robotic arm offers support to train the patient in real-life activities [27]. Additionally, the CAREN [28, 29] consists of a treadmill placed on top of the 6-DoF Stewart platform so that patients may experience perturbation from different angles while walking on the treadmill. However, due to the lack of sensory stimulation on the sole, weight transfer/pressure distribution training and personalization cannot be provided during PBT.

Prior to balance rehabilitation, it is very critical to improve the Range of Motion (ROM (plantar flexion/dorsiflexion, inversion/eversion, and abduction/adduction movements)) and proprioception and to measure somatosensory impairment levels so that the rehabilitation process can be tailored to the individual. There is no preparation phase in which these measurements are made in existing balance rehabilitation systems. In this context, systems in which the somatosensory disorders of individuals can be determined during the preparation phase are required. The robotic ankle platforms aim to improve this ankle preparation phase. There are different parallel manipulators designed with various DoF: the Rutgers ankle with 6-DoF [30], ARBOT with 3-DoF [31], CARR with pneumatic-driven motor and 3-DoF [32]. Unfortunately, the mentioned parallel manipulators lack haptic and force sensors in their end effectors, which limits the ability to measure pressure changes and provide haptic feedback input on the sole of the foot. Moreover, these platforms are not suitable for balance training after completing ankle proprioception rehabilitation due to their limited end effector area that can accommodate only foot and their low weight-bearing capacity. In addition, active participation is crucial in ankle and balance rehabilitation robots. Prolonged passive training, where the patient merely follows the robot's movements, has been shown to be ineffective in significantly enhancing brain plasticity and motor recovery [33, 34]. The "Assist-as-Needed (AAN)" approach, which adjusts assistance based on the patient's ability or task performance, is more effective. Research strongly supports that active participation promotes plasticity, so robotic controllers should intervene minimally to encourage patient involvement and recovery [35]. Therefore, training decisions with robotic devices should adhere to the AAN paradigm or impedance control to enforcement active force [36, 37]. However, most of the systems in the market are only able to perform passive training.

Apart from the external perturbation provided by a system, body movements such as stepping produce an internal perturbation. The Choice Step Reaction Time (CSRT) test is used to assess a person's ability to quickly trigger and complete a step action by self-perturbing the balance. During the test, the subject must step into one of the different targets placed straight and diagonally in front of him/her. This is used to explain and improve the relationship between APA parameters, stride length, and target distance during the transition from a static to a dynamic stance since stepping rehabilitation aims to enhance walking parameters, stepping accuracy, and the ability to step at various target distances [19, 38]. Fitts' law, which relates the time required to move to a target with the target's width and distance, is applied to understand motor planning in this context [11]. This law is used in the CSRT test to analyze the time it takes to complete a foot-reaching task and improve walking parameters. However, with these tests, the distance between the target positions and the starting point is changed manually instead

of the robotic/automatically adjustable distance. In addition, these targets only include a switch to measure reaction time and do not assess ground reaction force (GRF) for haptic feedback, limiting the ability to train patients in pressure distribution control. [11, 39].

The rehabilitation treatments used to improve motor skills and postural control based on the interconnection of sensory, cognitive, and motor processes; thus, the necessity for integrated training is increasing as well. Therefore, the Integrated Balance Rehabilitation (I-BaR) [6] framework is proposed in three phases, namely, ankle-foot, balance, and stepping. The ankle-foot/preparation phase aims to increase mobility, joint proprioception, and sole sensation. The balance phase aims to enhance sensory weighting abilities via PBT. Lastly, the stepping phase aims to enhance walking characteristics by performing stepping at adjustable-distance target points with internal/external perturbation.

In this study, we present the design of a novel BalanSENS system that is suitable for the I-BaR framework. In the first phase, ankle rehabilitation, the patient is seated on a chair while the ankle ROM, strength, proprioception, and sensory training are performed by the 3-DoF parallel manipulator. In the second phase, balance rehabilitation, sensory weighting skills are developed from motor learning by using multi-sensory input during PBT. Also, the support surface on the end effector of the parallel manipulator can be adjusted between 0-20^o, so that the difficulty of treatment can be changed during PBT. Furthermore, the system includes the haptic bar with this required upper limb support that can be measured. If the patients exceed their upper limb support threshold value and they are triggered with a vibration motor to use their lower extremities instead of relying on their upper extremities. In the last phase, stepping rehabilitation, according to the given signal, it is required from patients to step to the target points that are placed straight and diagonally with adjustable distance. The BalanSENS includes different sensors, e.g., vibration motors, load cells, IMU, and EMG so that throughout all phases, the measurements can be realized quantitatively and objectively. The system design is initially evaluated for the ankle passive preparation phase as a means of simulation and real-time characterization tests. The system design principles (sensor placement, servo motor specification, workspace restriction), designed electrical and load cell panels, and circuits are examined with these tests. As a result, it is proved that the system is suitable for the I-BaR protocol, and further prototypes of the system and I-BaR application are in our future work.

Table 1 Design criteria consideration [40]

Body parts	Minimum (mm)	Maximum (mm)
Height	1505	1855
Eye height	1405	1745
Sitting eye height	685	845
Knuckle height	660	825
Knee height	455	595
Hand breadth	70	95
Foot length	215	285
Body mass (kg)	44	100

This paper introduces a fully personalized rehabilitation system designed to patients with varying levels of severity or disorders, combining the three key phases of the I-BaR framework: ankle-foot, balance, and stepping rehabilitation. The study's originality includes:

- In the ankle phase, a customized therapy program is provided by identifying individual somatosensory disorders and delivering the necessary sensory information.
- In the balance phase, the system offers evaluation and training for static posture, proactive balance, reaction time, and reactive balance, all essential for postural control.
- During the stepping phase, the system assesses and enhances weight transfer capacity during the stance phase.
- The rehabilitation approach evaluates CoM, ROM, sole pressure distribution, and sole sensory input parameters.
- The Foot Rotation Angle (FRA) on the upper platform's foot plates is adjustable, i.e., ground support surface is adjustable so patients can participate with gradual improvement.
- The required upper extremity support by patients during PBT is calculated quantitatively with the haptic bar.
- Proprioception and somatosensory disorder levels are measured, allowing for a personalized rehabilitation plan.
- The chair is instrumented which means it includes load cell and vibration motor this will give the trunk movement during sitting activities and we can analyze the upper limb movement during all rehabilitation phases.
- The integrated balance rehabilitation process improves somatosensory information and weight transfer on the sole through haptic feedback.
- The system incorporates VR games to boost treatment continuity and effectiveness with sensory feedback.
- Multi-modal feedback is used to enhance sensory weighting skills.

2 BalanSENS design

The system should be developed to be comfortable for the user, adjustable, and available in various sizes. In this regards, requirements in the design process of the system, are given in Table 1. The lower and upper limits are

determined with the 5th and 95th percentile for female and male proportions, respectively, so that 95% of the user population would be compensated [40].

There are three different modules on the BalanSENS system (see Fig. 1a), which can be customized for different rehabilitation methods based on the patients' needs. The chair placement and the first step target points are included in the first module (see Fig. 1b, c) to be used in ankle-foot and stepping rehabilitation, respectively. In the second module, there is a parallel manipulator, to be used for two tasks. First, it can give perturbation (in ankle-foot and balance rehabilitation), and second, patients can use the end effector of the manipulator as the second stepping region. The third module includes the Virtual Reality (VR) setup, and the third step targets points. With this aim, our research proposes a completely personalized rehabilitation system for neurological patients with different severity levels. It integrates three main phases of I-BaR, i.e., ankle-foot, balance, and stepping rehabilitation. Each region and customization for the I-BaR protocol is detailed in Sects. 2.1, 2.2, and 2.3.

2.1 Ankle Rehabilitation

The first step module is removed during ankle rehabilitation, and a chair is placed in agreement with the ergonomic parameters (see Table 1, Fig. 1b, c). Hip-popliteal length, hip width, and shoulder height are some of the important parameters for personalized chair design criteria. Additionally, the distance between the knee, hip-popliteal, and parallel manipulator distance must be adjustable since each patient has a different body size. Similarly, the chair's height should have a range between 435–550 mm (see Fig. 1d) [40].

The 3-DoF parallel manipulator (see Fig. 1b) provides a dynamic environment during ankle and balance rehabilitation. It is equipped with three linear actuators mounted between the end-effector and the base of the robot. It is able to rotate in roll (α) and pitch (β) angles and moves along the z-axis. Roll and pitch are one of the most used angle changes by the ankle, and the elevation of the system in the z-axis also covers most of the active activities in real life. While the rotational adjustments in the roll and pitch axes are adequate for ankle movement, the translational shift along the z-axis also significantly impacts balance. These movements are also noticeable in many everyday activities, such as stepping, climbing stairs, and the recoil reactions generated by the feet. For instance, when ascending stairs, the body must adapt to the change in height with each step, requiring precise control over the z-axis movement to avoid imbalance. Similarly, plantarflexion/dorsiflexion movement enables a person to press a car's gas pedal or allows ballet dancers to stand on their toes. It involves the downward/forward motion of the foot away from the body and plays a key role in actions that require pushing off the ground. Inversion and eversion, on the other hand, help the foot adapt to various surfaces and terrains, whether walking on uneven ground, climbing stairs, or running on a track. The combination of these foot movements with the z-axis elevation is vital for maintaining stability and balance during dynamic activities. These coordinated movements ensure effective propulsion and balance, whether adjusting to changes in height while climbing stairs or adapting to different

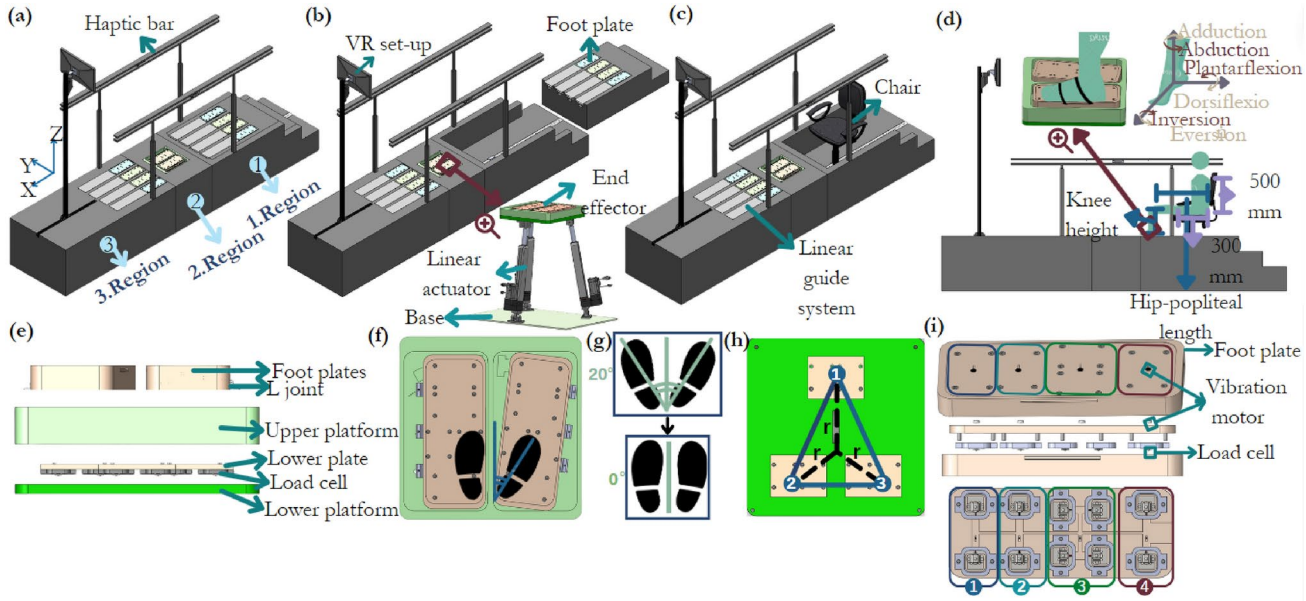

Fig. 1 Representation of **a** BalanSENS, **b** the removal of the 1. region, **c** chair placement, **d** ankle rehabilitation set-up, **e** end effector layers, **f** top view of upper platform, **g** foot rotation angle-support area relationship, **h** top view of lower platform, and **i** foot plate detail

surfaces while walking or running. The interplay between rotational and translational movements is essential not only for everyday activities but also for more complex tasks that demand greater balance and coordination, detailed design motivations are explained in our previous work [41]. These DoFs are chosen to provide mechanical simplification of the system while providing quality PBT. The ankle ROM (see Fig. 1d) is limited with 0-20^o dorsiflexion, 0-50^o plantarflexion, 0-10^o adduction, 0-5^o abduction, 0–20^o eversion and 0–35^o inversion [42]. While in therapy, upper limits are determined according to the severity levels of the patient and are gradually increased to the maximum limit based on their performance. Thus, ankle ROMs and proprioception are improved gradually (I-BaR specification in Fig. 2a ROM section).

The end effector of the parallel manipulator (see Fig. 1e) is designed as a two-layer structure retaining multiple load cells and vibration motors. The upper platform (see Fig. 1f) is responsible for evaluating the pressure obtained from the soles of the feet. There are two separate foot plates (see Fig. 1f–i) for the right and left feet on the upper platform. Each foot plate is divided into four regions, i.e., toes, metatarsals, middle foot, and heel. These regions are known as the more weight-bearing regions on the feet and are used as a reference when determining the placement of the load cells [43]. Furthermore, it is indicated that 43% of patients have decreased sensations in their soles [44]. For these reasons, as shown in Fig. 1i, vibration motors are placed on each of the regions. These motors are activated if the patient's weight transfer/pressure is insufficient during proprioception training. With this feedback, the patient can sense the amount of weight transfer and pressure on their soles and be trained to transfer their weight correctly to prevent falls. This feedback specification and VR environment can be used in ankle rehabilitation as multi, uni, and no feedback option (for the I-BaR ankle specification, see Fig. 2A Feedback section).

2.2 Balance Rehabilitation

The 3-DoF parallel manipulator (see Fig. 1b) can measure reaction time, pressure distribution, and CoM. Thus, the platform provides a quantitative assessment of patients' balance ability and their cognitive responses to compensate for the impaired balance against the perturbations with various tasks and multiple motor inputs. As in Sect. 2.1, the platform movement initiates with a limited ROM, and as the level progresses, the angular deviation increases up to the maximum ankle anthropomorphic. Thus, once patients begin to control the preliminary minor perturbations, they can balance the major perturbations better (see Fig. 2b ROM section limit).

The Foot Rotation Angle (FRA) on the upper platform's foot plates is adjustable between 0–20^o (see Fig. 1f-g). As the angle between the FRA decreases, the movement becomes more difficult due to the decrease in the support surface. In balance rehabilitation, the foot rotational angle value gradually reduces as shown in Fig. 2b support surface specification so patients can participate with gradual improvement. The lower platform (see Fig. 1e-h), located just below the upper platform, is responsible for evaluating patients' CoM. The necessary data for calculating the CoM of the body in the x-y coordinate plane are obtained through three load cells positioned at the vertices of a equilateral triangle located on the lower platform, as depicted in Fig. 1h. The CoM is subsequently computed using Eqs. 1 and 2 as each corner weight is calculated with its corresponding weight on the load cell and r represents the distance from each vertex to the centroid of the equilateral triangles. This instantaneous CoM measurement can be useful to provide feedback to the control architecture to determine the patient's postural control capacity and adjust the level of assistance.

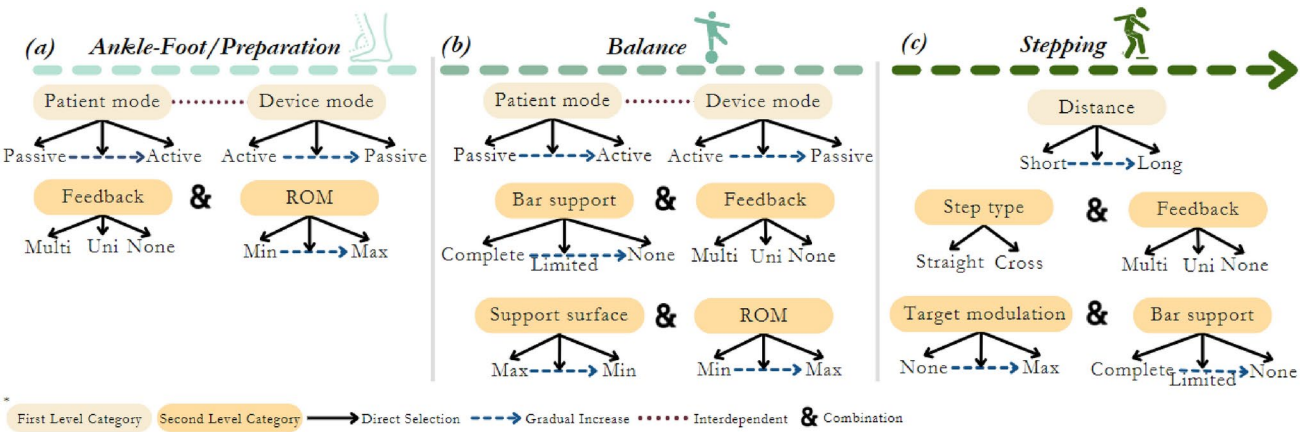

Fig. 2 I-BaR protocol with BalanSENS

$$COM_x = \frac{(weight1)r - (r\sin(30^o))weight2 - (r\sin(30^o))weight3}{weight1 + weight2 + weight3} \quad (1)$$

$$COM_y = \frac{(r\cos(30^o))weight2 - (r\cos(30^o))weight3}{weight2 + weight3} \quad (2)$$

The required upper extremity support by patients during PBT is calculated quantitatively with the haptic bar, which contains load cells and vibration motors (see Fig. 1c). The width of the haptic bar is designed according to the hand width of an average person (for ease of grasp), and their height can be adjusted according to the needs of the patients (600–900 mm) [40]. First of all, patients with high balance loss are asked to balance their CoM during PBT with the complete help of haptic bars. As the patient's postural control improves, an upper extremity support threshold value is determined for each individual and is constantly updated during rehabilitation (see Fig. 2b Bar Support). If the patient exceeds the threshold, haptic feedback is applied to reduce the upper limb support and regain their balance by using their lower limb. As patients progress in their balance capacity during rehabilitation, they are asked to receive upper limb support only when necessary. Consequently, it is intended that they use their affected lower limb rather than relying on the upper limb.

2.3 Stepping Rehabilitation

While walking rehabilitation primarily aims to enhance muscle contribution and activation during continuous walking, stepping rehabilitation focus diverges. Its objective is to enhance the patient's decision-making process rather than directly improving their walking performance. Stepping rehabilitation is used to enhance the ability to step over specific target distances, step accuracy, and gait characteristics. Furthermore, while treadmill-based balance rehabilitation proves beneficial for individuals with higher impairment levels, the focus on stepping rehabilitation caters to a different demographic. Specifically, stepping rehabilitation's target group comprises individuals capable of walking but exhibiting slower reactions and sensory processing.

The modifiable stepping target points are essential since variations in APAs, and muscle and strength duration are influenced by task distance: the more challenging the task, the later postural muscle activity begins. Particularly, at stepping long distances, patients realize the movement faster with their own compensation strategies, which reduces the quality of motion, whereas at stepping short distances, their motion is slower, controlled, and precise. This compensation can be assessed with BalanSENS by analyzing the relationship between muscle activity (EMG), postural control (CoM deviation control), movement speed, and accuracy (weight shift and pressure distribution). Moreover, previous research on balance control has shown that adopting an external focus of attention compared to an internal focus of attention results in better performance during motor skills [11]. For the reason stated, the external starting signal can be provided visually with VR and auditory with a sound warning in stepping rehabilitation. The warning selection can be made as multi, uni, and no feedback option (see Fig. 2). The distance between the stepping locations can be modified between 15–75 cm (as seen in Figs. 2c and 3a, b) better to comprehend the correlation between movement speed and accuracy.

Foot plates are strategically positioned on designated target points, enabling the calculation of Ground Reaction Force (GRF) and providing haptic feedback as an additional external signal in cases where patients are unable to initiate a step following the initial external signal. The muscle activity is determined according to two measurement parameters: the time window between the onset of the muscle activity measured by wireless and mobile EMG service and the through-the-movement kinematics. The BalanSENS incorporates a linear guide system for adjusting the position of the target points. The utilization of the linear guide system presents an additional benefit by introducing perturbations during the patient's progression toward the target points, facilitating a dynamic rehabilitation approach that closely emulates ADL. The velocity of these perturbations can be customized based on the severity level of the patient, allowing for personalized rehabilitation interventions.

2.4 Wearable Sensors

One of the most beneficial rehabilitation techniques is task-oriented training that provides feedback from various sensory inputs, such as pressure, vibration, and proprioception [2]. These inputs aid in overcoming the loss of motor function caused by the damaged neuromuscular system by developing compensating mechanisms and strategies. During rehabilitation, the specific EMG placement should be adjusted with the help of a physiotherapist for each patient. Still, the data measured by focusing on the important muscle groups, the tibialis anterior, medial gastrocnemius, rectus femoris, biceps femoris, and gluteus medius, provide valuable information about the patient's performance. One way to address this problem is with Vibrotactile Feedback (VF) [45] since it provides haptic stimuli to the points where the loss of sensations and triggers the required region. That's why, VF rings are placed on the patient. If the patient's muscle activity is decreased and delayed (which is measured with wireless and mobile EMG service), VF rings starts stimulate/trigger the patient's responsible muscle groups through a feedforward signal. That's why, VF rings (see Fig. 3c–e) are placed on the patient. If the patient

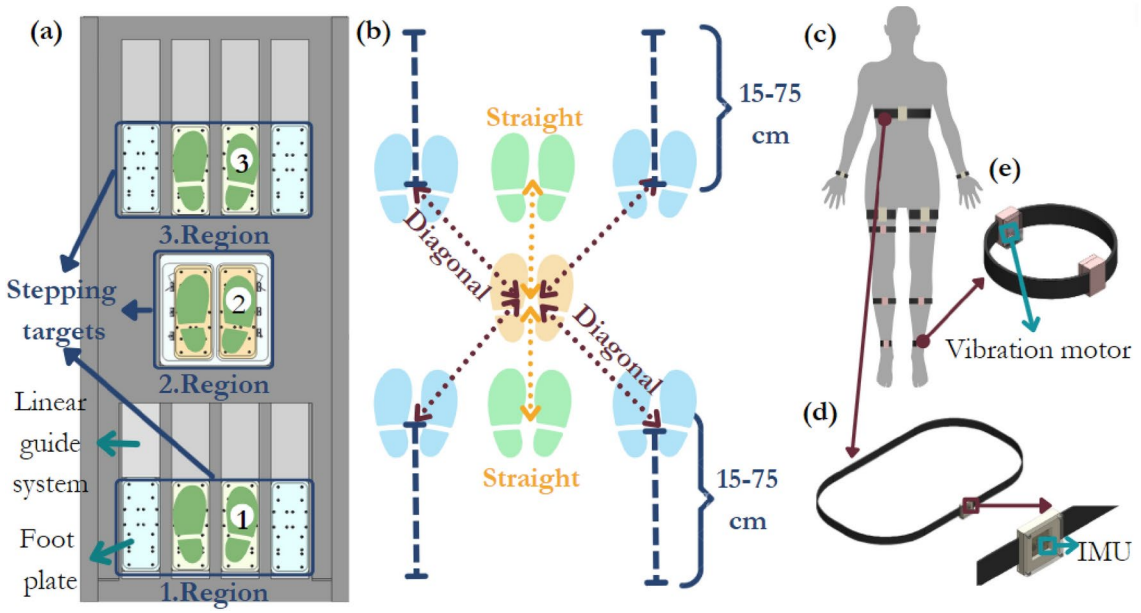

Fig. 3 Representation of **a** step rehabilitation set-up, **b** stepping measurement process, **c** Wearable sensor placement, **d** IMU embedded ring, and **e** Vibration motor embedded ring

does not show muscle activity (measured with wireless and mobile EMG service), VF rings are used to stimulate/trigger the patient's muscles with a feedforward signal. In these rings, the vibration motor is placed around the soft tissue and attached to a belt so it is not in direct contact with the patients, and the diameter of the ring can be adjusted. The frequency of vibration motors should be determined by the individual's sole of the feet sensation. To achieve this, the range between 100 Hz and 200 Hz should be divided into five equal intervals and then tested on the patient. Based on the first feedback, the personalized vibration motor frequency can be determined by conducting at least five trials within the selected interval that aligns with the individual's response. Similarly, postural sway is evaluated by measuring the trunk, arms, and legs of the patients by Inertial Measurement Unit (IMU) ring (see Fig. 3c, d).

3 Simulation Analysis

The kinematic and dynamic analyses of the proposed 3-DoF parallel manipulator are based on closed-loop kinematic equations and the Lagrangian method, respectively. As a result, the angular equations and relations for the physical variables of the mechanism are presented in our previous work [41].

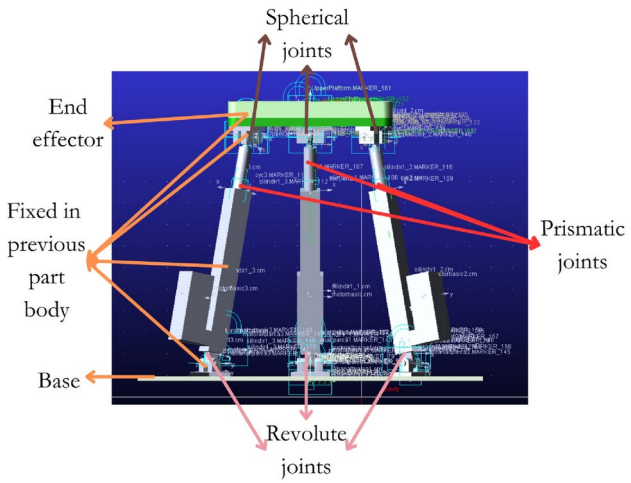

Fig. 4 ADAMs simulation model

3.1 ADAMS Analysis

The ADAMs program analyzes the velocity, position, force, and torque values that are derived from the kinematic and dynamic equations. The determined force/torque values are used when deciding on the linear actuator. After the model is transmitted to software (see Fig. 4), the joint type is assigned to its corresponding part (Spherical, prismatic, revolute and fixed). Then, the external force applied on the model to see what is the applied force on each actuator during each motion.

The parallel manipulator has 3-DoF (rotations in roll and pitch directions and linear translation in the z-axis) and includes three linear actuators. Each actuator acts in

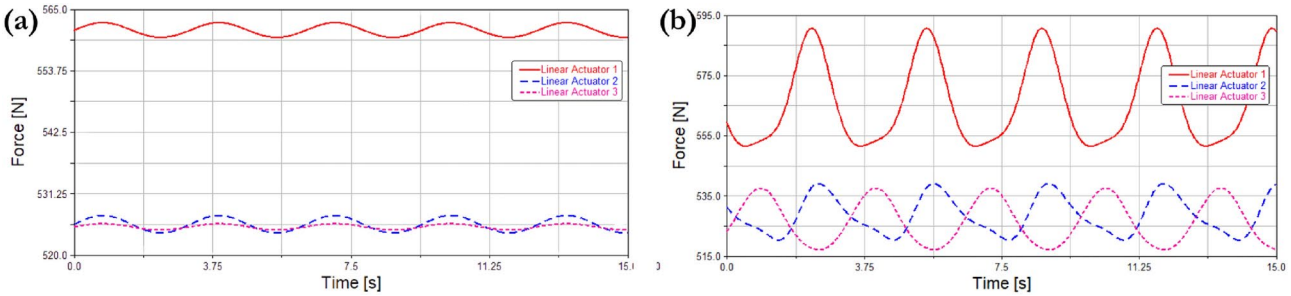

Fig. 5 **a** Required forces at z translation and **b** at circle motion

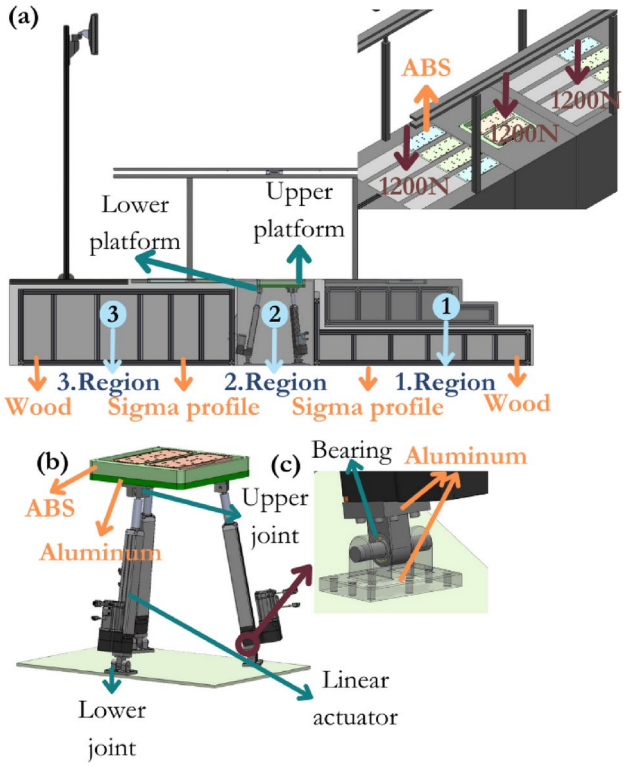

Fig. 6 Material selection on **a** All system, **b** 3 DoF parallel manipulator, and **c** Motor joint

accordance with different references after controllable DoFs (rotation in roll and pitch and z translation) is given as a reference constraint equations are used to solve the yaw rotation and x and y translation; the detailed structure is expressed in our previous study [41]. Therefore, the positions of the motor movements to be given in the simulation are found by using inverse kinematics equations in MATLAB, and then the obtained function is written in the ADAMs program. Two motion is shown as an example; the first one is for the solely z-translation in this motion, all actuators are moving in the same direction, but the maximum force is found as 568 N in the first linear actuator (end effector is not symmetrical thus load distribution creates this difference), as depicted in Fig. 5a. Similarly, in the second motion for the circular motion of the end effector in this motion all actuators work against each other so the force requirement is highest. The first linear actuator demonstrates a maximum required force of 1350 N, as shown in Fig. 5b, and servo motor capacity is chosen accordingly.

3.2 ANSYS Analysis

The feasibility of the designed system, the safety of the person on the device, and the reaction of the device under static stress are evaluated in ANSYS program (see Fig. 6). Thus, the stress, displacement, strain, and durability of the system are tested. Simulation is performed with summation of the maximum human weight limit and end effector weight. The material selection criteria are stiffness, strength, toughness, lightweight, and cost (see Fig. 7). The weight of the patient is distributed to foot plates, load cells, and lower platform, so these parts must have a high young modulus. Among the metallic materials considered, aluminum emerges as the optimal choice due to its lightweight nature and high modulus, ensuring both durability and minimal strain on the linear actuator. Furthermore, since the patient does not directly apply force on the frame of the upper platform, ABS is chosen as its material. The peak values of the result indicate that the compression force leads to a deformation of less than 1 mm, which is considered negligible and confirms the system is rigid and durable.

3.3 Simscape Analysis

Simscape analysis is used to verify the structural interaction of the selected material and control of linear actuator because the dynamic model of the 3-DoF parallel manipulator is composed of nonlinear functions of the state variables (Fig. 8), i.e., mass matrix, centrifugal and Coriolis matrix, gravity vector, forward and inverse kinematics [41]. This characteristic of the dynamic model makes the closed-loop control system nonlinear and difficult to solve. Computed Torque Control (CTC) is specifically useful for parallel manipulator types since its additional second loop leads to feedback linearization (see Fig. 9). The proposed parallel manipulator is modeled using the multibody library

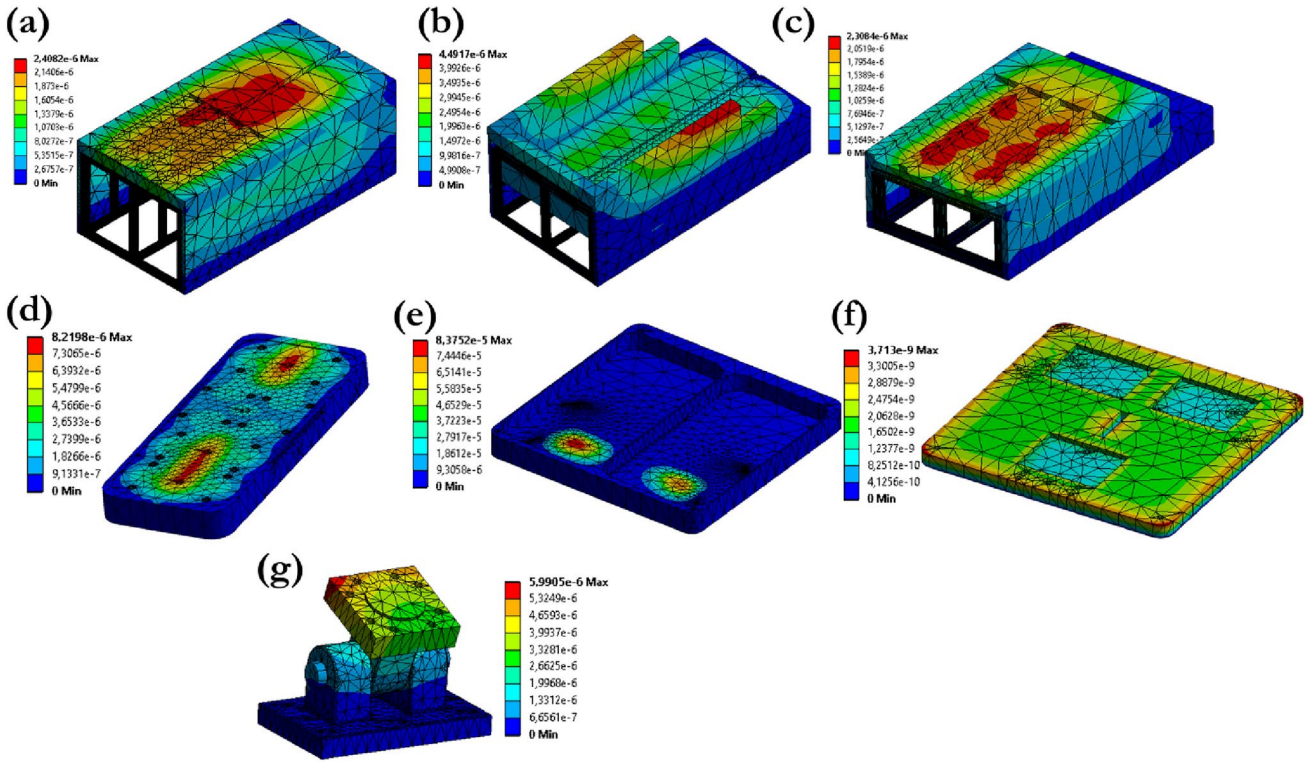

Fig. 7 Total deformation of **a** 3rd region, b 1st region lower part, **c** 1st region upper part, **d** Foot plate, **e** Upper platform, **f** Lower platform, and **g** Motor joint

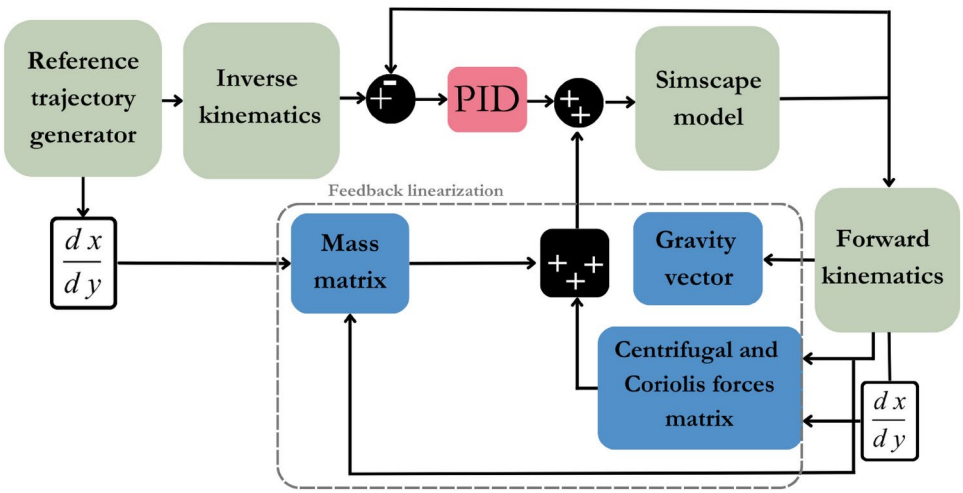

Fig. 8 Computed torque control simulation model

in Simulink. The physical attributes of each solid component, including inertia, mass, material, and geometry, are extracted from CAD model files. Then, parts were added to each other with frame transformation. Prismatic joints are defined in the piston part of linear actuators and force is given as input and the position of the joint is measured (see Fig see. Figure 9b each link is placed in green (first), blue (second), and yellow (third) colored areas). Then, the CTC simulation of linear actuators in a dynamic environment is evaluated. The end effector can rotate in roll and pitch angles and translation in the z-axis or combination between these axes. The Root-Mean-Square Errors (RMSEs) of the position tracking results of 4 different end effector references are summarized in Table 2. Even though the RMSE value is similar to each other, the maximum one on the first actuator in z-translation motion.

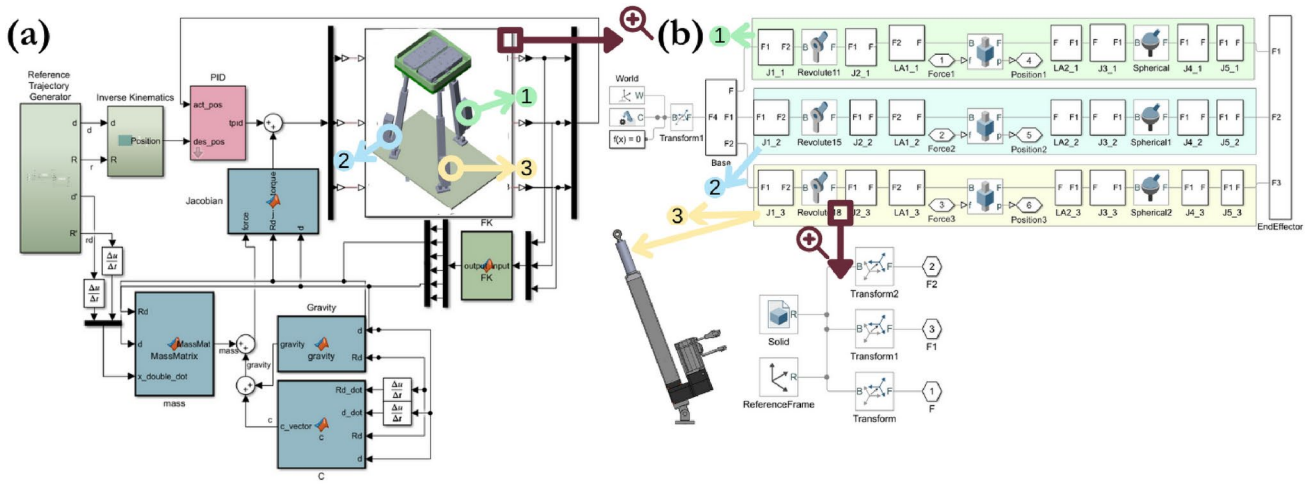

Fig. 9 **a** Computed torque control simulation and **b** Simspace Model of the parallel manipulator

Table 2 RMSE of linear actuators position tracking in Case 1: Translation in z, Case 2: Rotation in x and y, Case 3: Rotation in y, and Case 4: Rotation in x

Actuator number	Case 1	Case 2	Case 3	Case 4
Actuator 1	3.006 x 10−^{6}	3.004 x 10−^{6}	2.982 x 10−^{6}	2.998 x 10−^{6}
Actuator 2	2.814 x 10−^{6}	2.777 x 10−^{6}	2.982 x 10−^{6}	2.706 x 10−^{6}
Actuator 3	2.077 x 10−^{6}	2.123 x 10−^{6}	2.982 x 10−^{6}	2.202 x 10−^{6}

4 Real-Time Analyses

The 3 DoF robotic manipulator prototype is built, and its design characteristics are evaluated during the passive ankle preparation phase. While the system comprises various components, the primary focus was on the dynamic aspect, specifically the 3-DoF parallel manipulator, because since this is a parallel manipulator, an error in the connection prevented the prototype of the entire system. In addition, the same foot plates that have been used in the parallel manipulator's end effector are also used in the stepping targets by testing their data acquisition, a general structure can be obtained.

The manipulator's sensors and motors are connected to two panels, namely the electrical and load cell panels (see Fig. 10, for their connection scheme, see supplementary material). The electrical panel comprises of computer

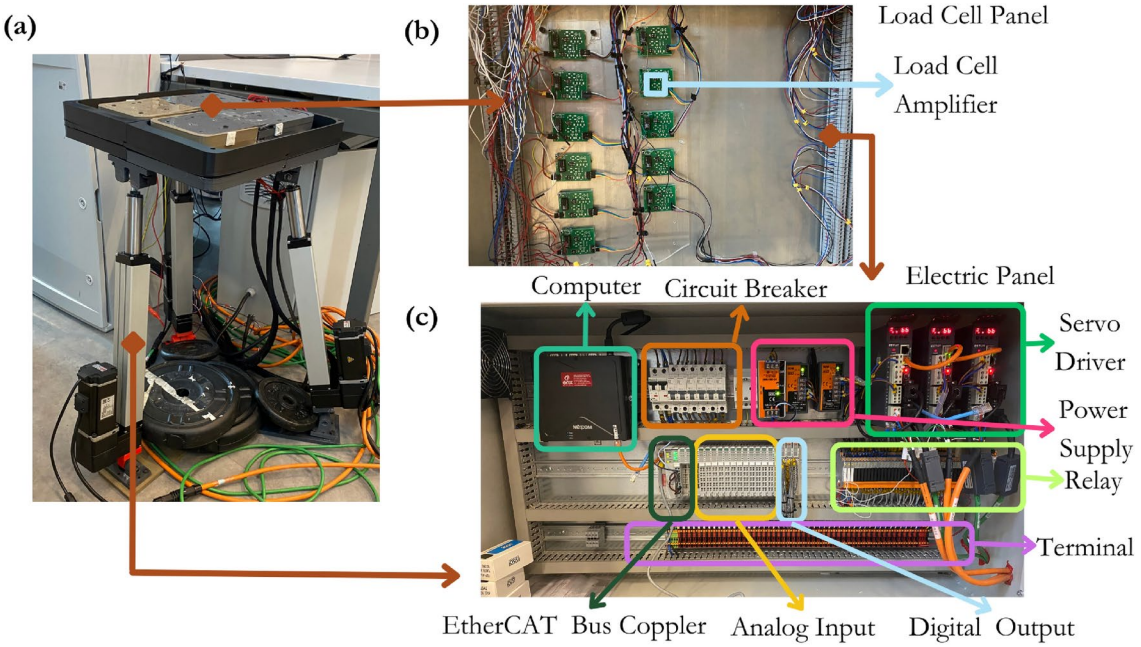

Fig. 10 **a** The first prototype of the designed parallel manipulator, **b** Electrical and **c** Load cell panel

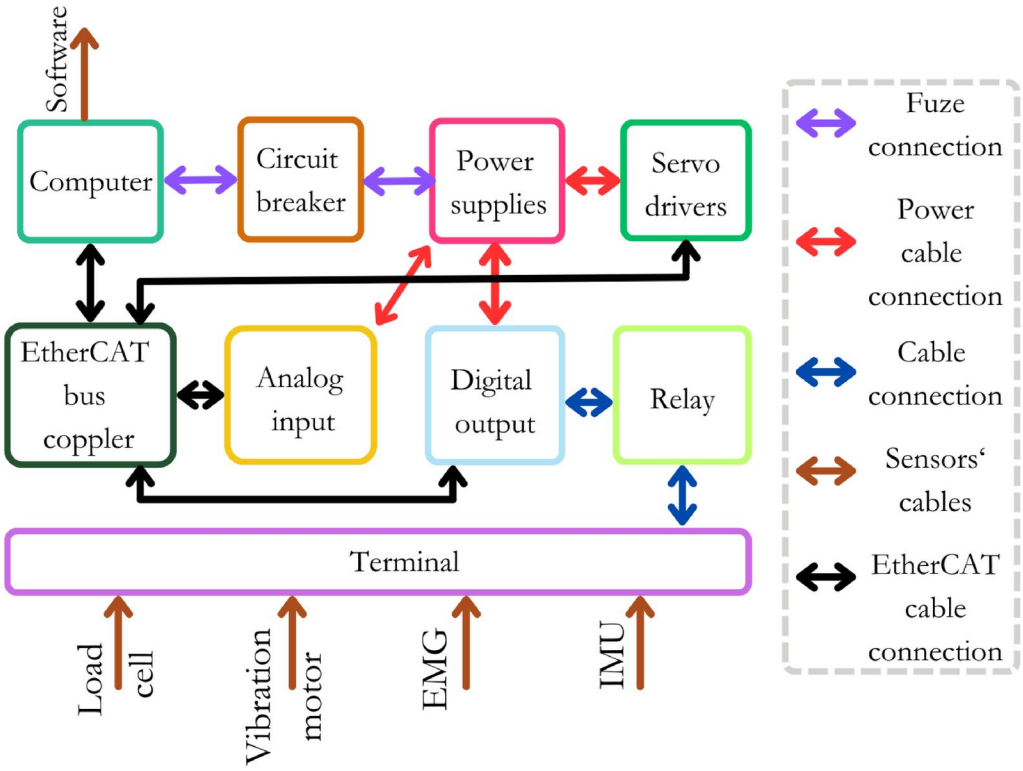

Fig. 11 Electrical panel connection scheme

(NISE 50-J1900 (Intel Celeron processor J1900 quad Core, 2.42GHz, 8 GB RAM)), circuit breaker, power supplies, servo driver (Estun Pronet-04AEG-EC), Solid State Relay, Terminal, Analog Input Module (CREVIS GT-3424), Digital Output Module (Crevis GT-226F), and EtherCAT Network Adapter (Crevis GN-9386). CodeSyS software is used to facilitate the coordination and exchange of data between hardware modules and software applications. The load cell panel only includes the designed load cell amplifier circuit, and outputs from these circuits are connected to the analog input module in the electrical panel. The amplifier circuit is designed with a notch filter to eliminate the 50 Hz power line noise. The load cell amplifier is simulated in the LtSpice software to ensure that the notch filter can remove the 50 Hz noise signal. Then, the Printed Circuit Board is designed on EAGLE software (for circuit design and simulation, see supplementary material).

4.1 Electrical Panel

The robotic platform design includes a large number of sensors (load cell, vibration motor, IMU, and EMG); that's why, in the long run, in order to solve communication problems, the manipulator's sensors and motors are connected to two panels, namely the electrical and load cell panels. The internal wiring of the electrical panel is made among itself, and its connection to the outside is left only with the workstation and sensor cables. All outside sensor cables are connected to the terminal. They are not connected directly to other components because output cables can be removed easily if something goes wrong with a sensor. Load cell cables are connected to the terminals, and then corresponding cables go to analog input modules to transmit the data to the computer with EtherCAT Bus Coppler. Similarly, vibration motors terminal connections' are connected to relays, and then relays are connected to digital output modules. If the vibration motors need to be triggered according to the data received from the load cell or EMG, the digital module will trigger the relays, ensuring that they are short-circuited, thus enabling the vibration motors to become active by passing current through them.

4.2 Load Cell Panel

The load cell panel (see Fig. 12) only includes the designed load cell amplifier circuit, and outputs from these circuits are connected to the analog input module in the electrical panel. Only the load cells in the parallel manipulator have been connected (11 units). In future testing, other load cell amplifiers also will be connected.

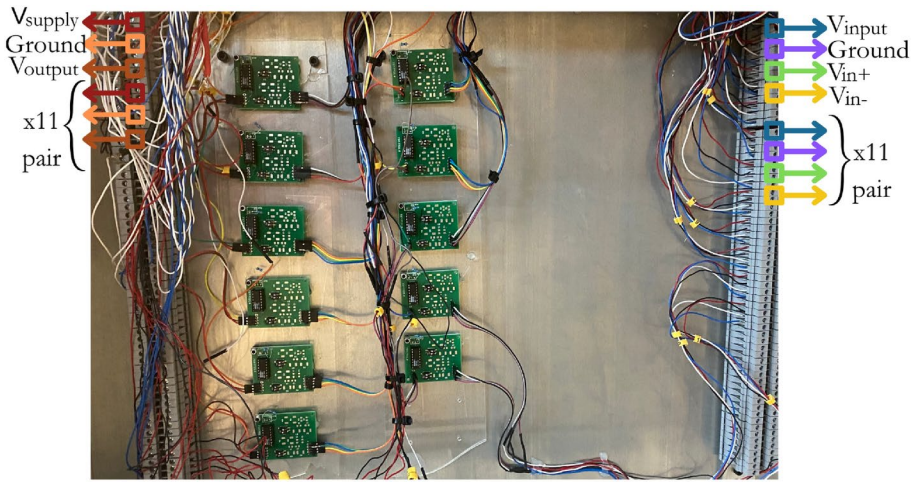

Fig. 12 Load cell panel connection scheme

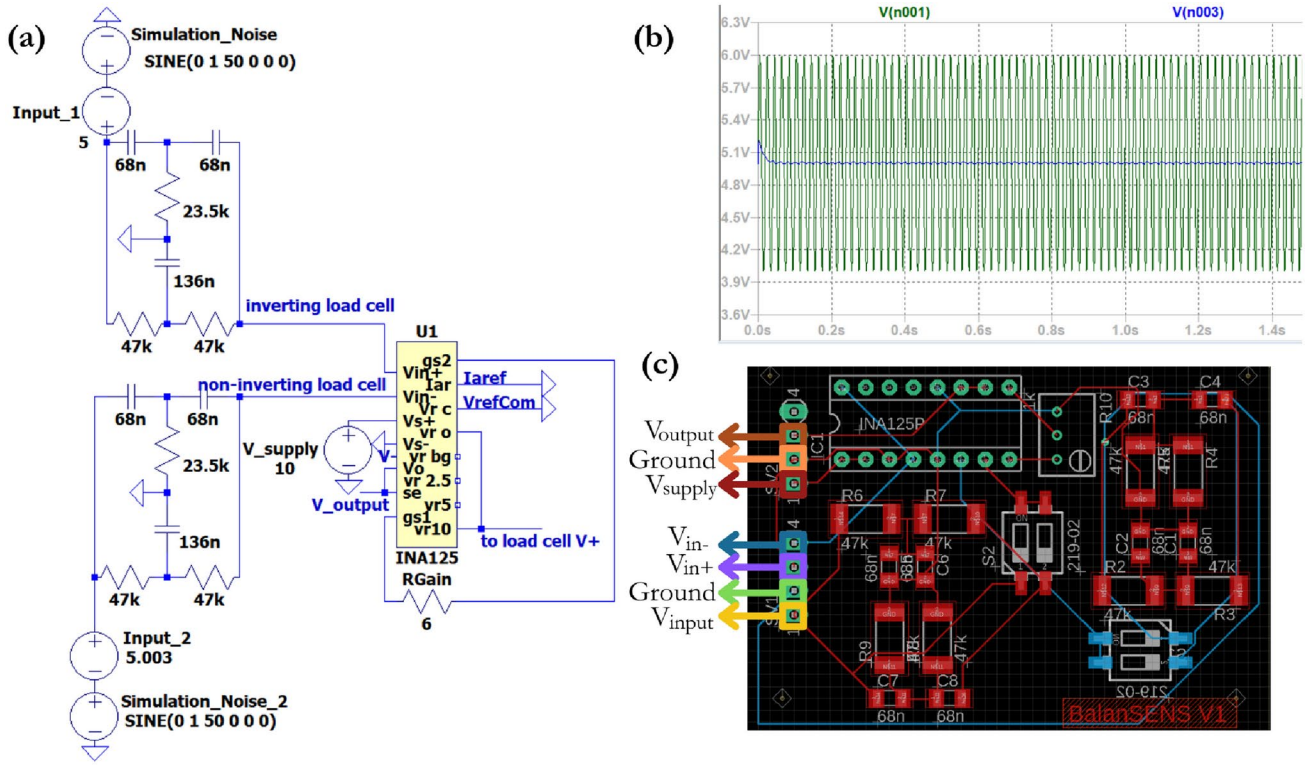

Fig. 13 **a** LtSpice simulation, **b** simulation result, and **c** PCB design of load cell amplifier

4.3 Load Cell Amplifier Design

Load cells are force transducers that convert force to electrical signals. They are made of strain gauges in a Wheatstone bridge position. The strain gauge's wire or foil is designed to vary resistance when force is applied. The signal's amplitude varies in direct proportion to the force exerted. However, it is hard to detect voltage changes accurately since the change in resistance is observed in millivolts by using amplifier circuit minor differences can be magnified into more detectable signals. Load cells have four cable voltage supply (Vinput), ground, inverting (Vin+) and non-inverting (Vin-) inputs. They are connected to the PCB and supply and ground directly connected to the Integrated Circuit's (IC)(INA125) supply (Vsupply) and ground. Similarly, inverting and non-inverting signals are connected to the notch filter then filtered signals are connected to the IC. The amplified output (Voutput) connected to the analog module in the electrical panel. Before this circuit (see Fig. 13c) was produced, the circuit was simulated in the LtSpice program (see Fig. 13a). PCB was produced after observing that the

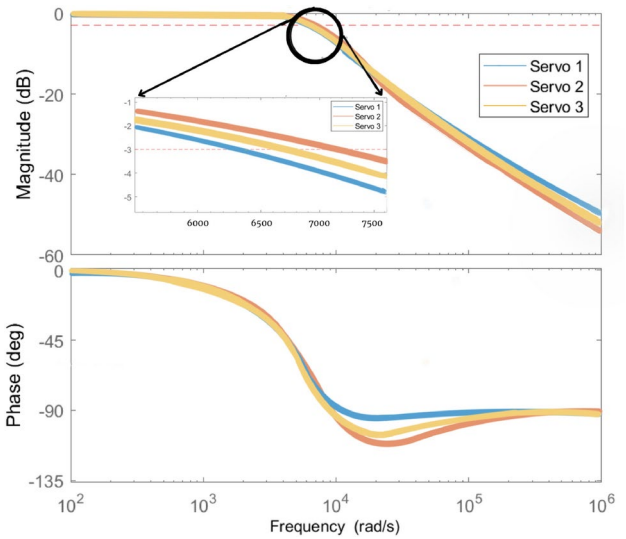

Fig. 14 Frequency response characteristics of the servo motors

notch filter can minimize the noise signal in the simulation (see Fig. 13b).

4.4 System Characterization

The system's dynamic behavior and the motor's performance characteristics are assessed by analyzing various frequencies in the Bode plot. To examine this, a chirp signal (initial frequency starting at 10 Hz and ending at 1 kHz for 120 s.) is generated on the software and employed as a reference input for the servo motor (while the system is in assembly form). Subsequently, the collected data and the references are utilized in the MATLAB system identification toolbox to ascertain the corresponding transfer functions for each servo motor. Following this, the Bode plots are obtained, displaying the gain and phase shift of the servo motors. This finding is particularly crucial in designing and implementing control algorithms, as it helps select appropriate limits in rehabilitation [6]. The result shows that frequencies up to 6300 Hz (see Fig. 14) have high gain, and motors are controllable. In addition, even though the second and third servo motors have higher cutoff frequencies since they all are to be controlled with the same frequencies, the lowest one is taken as the limit. The phase plot of servo motors' shows the time delay between the input and output signals. It does not exceed -180 degrees thus, the open loop response of the servo motors does not operate near the instability region in the I-BaR requirements [6].

The characteristics of servo motors are identified through a series of tests by velocity, accuracy, and response time as the same 3 DoF platform will be used in the all rehabilitation process servo motor response in real-time is important. Thus, different position (10 to 100 mm) and velocity (10 to 100 mm/s) inputs are analyzed to see the motors' insights into the performance and behavior of the servos under different operating conditions. By analyzing the characteristics of the servo motors, their control capacities are proven for the I-BaR application [6], ensuring reliable and precise control in the system.

The system is tested with different velocities (from 10 to 100 mm/s as set to be rehabilitation limit references) and target distances (from 10 mm to 100 mm is set to be the range in z translation) with a 2 ms sampling rate with five repetitions for each motion. As shown in Fig. 15, in

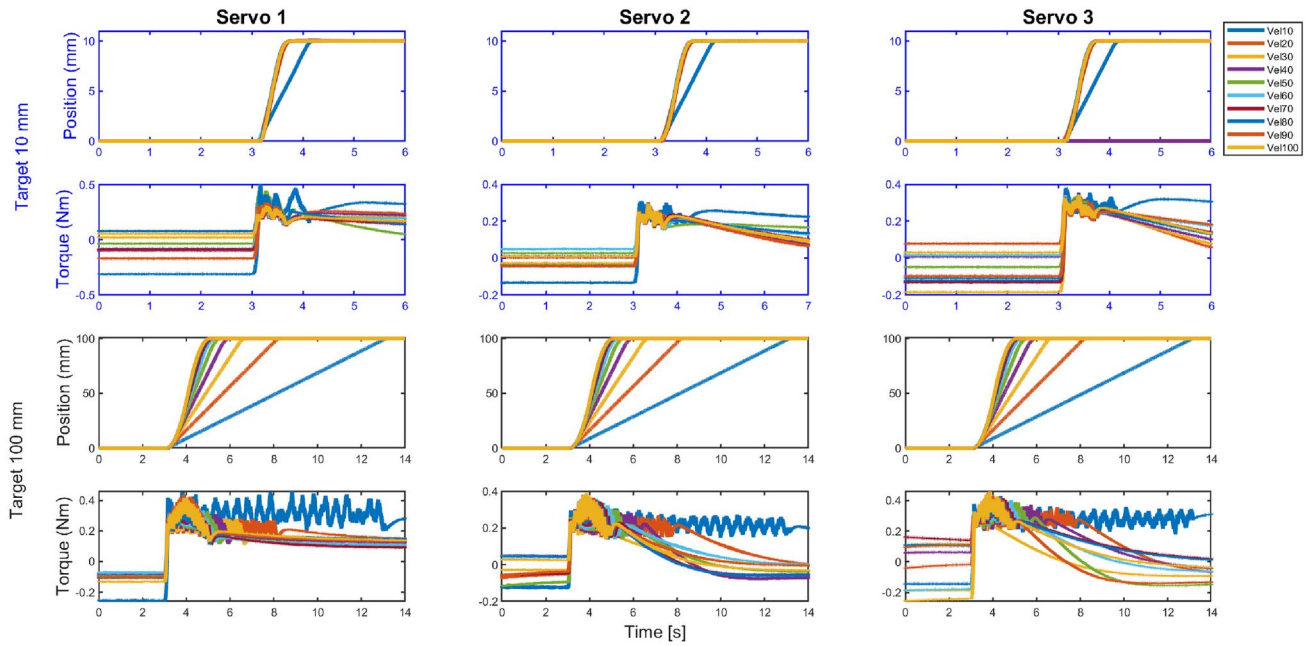

Fig. 15 Servo motors position and torque tracking characteristics on low and high velocity

Table 3 RMSE, rise and settling time for different conditions

Servo motor, reference position and Reference velocity, respectively	Rise time [s]	Settling time [s]	RMSE [mm]
S1, Position 10 mm, Velocity 10 mm/s	0.942	2.172	0.110
S1, Position 10 mm, Velocity 100 mm/s	0.484	1.488	0.136
S1, Position 100 mm, Velocity 10 mm/s	9.039	11.261	0.281
S1, Position 100 mm, Velocity 100 mm/s	1.534	2.678	0.773
S2, Position 10 mm, Velocity 10 mm/s	0.942	1.750	0.100
S2, Position 10 mm, Velocity 100 mm/s	0.510	0.784	0.137
S2, Position 100 mm, Velocity 10 mm/s	9.043	10.489	0.276
S2, Position 100 mm, Velocity 100 mm/s	1.550	2.576	0.772
S3, Position 10 mm, Velocity 10 mm/s	0.932	1.992	0.107
S3, Position 10 mm, Velocity 100 mm/s	0.480	0.754	0.135
S3, Position 100 mm, Velocity 10 mm/s	9.031	11.507	0.277
S3, Position 100 mm, Velocity 100 mm/s	1.534	2.634	0.773

the lowest target position (10 mm), velocities do not show a significant difference, whereas, in the highest target position (100 mm), the differences become more evident (rise time decrease, and torque response and accuracy increase) as velocity increases. Table 3 summarizes the servo motor response at its lowest and highest value. The longest rise and settling time obtained as 9.039s and 11.261s, 9.043s and 10.489s, and 9.031s and 11.507s for the first, second, and third servo motor, respectively, with the reference to go to the 100 mm position target with 10 mm/s. Whereas the highest amount of error time is obtained as 0.773mm, 0.772mm, and 0.773mm for the first, second, and third servo motor, respectively, with a reference to go to the 100 mm position target with 100 mm/s. Detailed explanations about different position targets and velocities have been provided in the supplementary materials file.

4.5 Design Evaluation

The robotic platform design are evaluated by a series of experiments with one healthy subject; five repetitions of each experiment trial for 3 min with a 2 ms sampling rate are realized while the subject's feet are placed on the prototype. The studies involving human participants are reviewed and approved by the University Research Ethics Council of Istanbul Medipol University under the E-66291034-772.02-4494 number. The participant provided their written informed consent to participate and data sharing in this study. The design testing is performed on one of the authors without a formal recruitment process, i.e., the recruitment period is not used in this paper. The experimental evaluation started on 15 May 2023 and ended on 29 May 2023.

The design evaluation tests are conducted to evaluate the protocols between servo motors, panels, and computer programs. The aim was to test the system's capability to transmit data efficiently and accurately in real-time experiments between panels.

Table 4 Weight measurement of the subject's feet while the end-effector is in z-translation, roll, and pitch motion

Load cell number	Z-translation [kg]	Roll [kg]	Pitch [kg]
LC 1	1.297 ± 0.040	1.264 ± 0.066	1.218 ± 0.086
LC 2	0.469 ± 0.108	0.373 ± 0.094	0.556 ± 0.167
LC 3	0.603 ± 0.086	0.402 ± 0.063	0.799 ± 0.165
LC 4	1.048 ± 0.060	1.779 ± 0.096	1.917 ± 0.177
LC 5	1.089 ± 0.060	1.089 ± 0.085	1.276 ± 0.098
LC 6	0.487 ± 0.033	0.480 ± 0.025	0.497 ± 0.026
LC 7	0.467 ± 0.048	0.493 ± 0.075	0.453 ± 0.050
LC 8	1.798 ± 0.119	1.921 ± 0.250	1.947 ± 0.146

These tests aimed to evaluate the device's effectiveness/limits in facilitating the ankle preparation phase and its sensor communication between the electric and load cell panels. Each trial involved specific sets exercise (subject passively placed her feet in the system), i.e., end effector rotation in roll and pitch and translation in z movements, then with the inverse kinematic equations (explained in [41]), corresponding servo motors' positions are found and used as the reference trajectory.

Understanding the dynamic interaction between the servo motors and load cell sensors is crucial for ensuring the manipulator's accurate control and reliable operation (between the load cell and electrical panels). Thus, the load cells, servo motor position tracking, and end effector orientation data throughout the rehabilitation process are analyzed during each reference orientation (roll, pitch, and z limits). The servo motors were effectively manipulated to attain their intended positions by employing specific end effector references (roll, pitch, and z) through the utilization of inverse kinematic equations. Subsequently, the measured end effector's value is obtained from forward kinematic equations with linear actuators encoder data. The comparison between the values derived from these forward kinematic equations and the reference values is the first 10-second values represented in Fig. 17. While the first two columns show the end effector orientation and position of the load cell during roll movement, the two in the middle show during pitch motion, and the last two show the movement in the z-translation. This comparison shows the alignment between the referenced orientation and the measured results. Servo Load cells experimental trials' mean and standard deviation have been presented in Table 4. The detailed analysis of each movement has been provided in the supplementary materials file. The first 15-second values of the data collected for each load cell are presented in the Fig. 16 during each motion. While the first two columns show the measurement of load cell during roll movement, the two in the middle show during pitch motion, and the last two

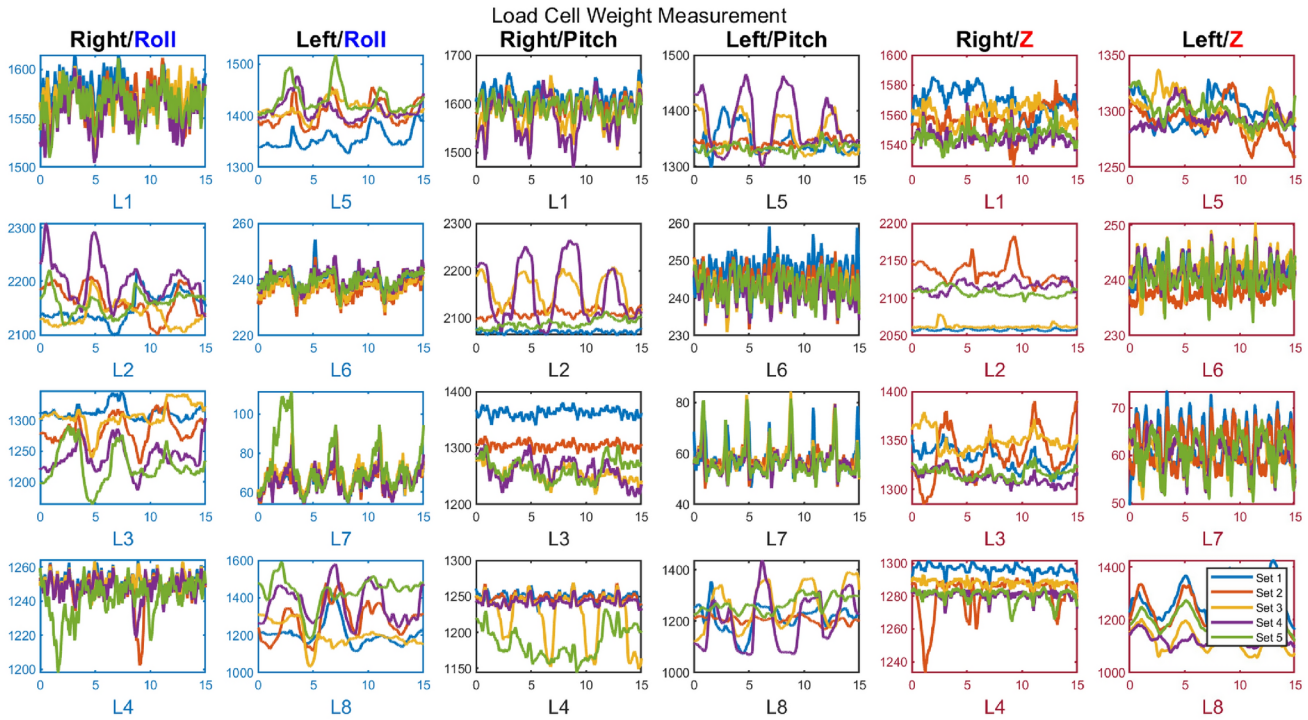

Fig. 16 Load cell measurements during design testing (Blue, black, and red color text represents roll, pitch, and z-translation movement, respectively)

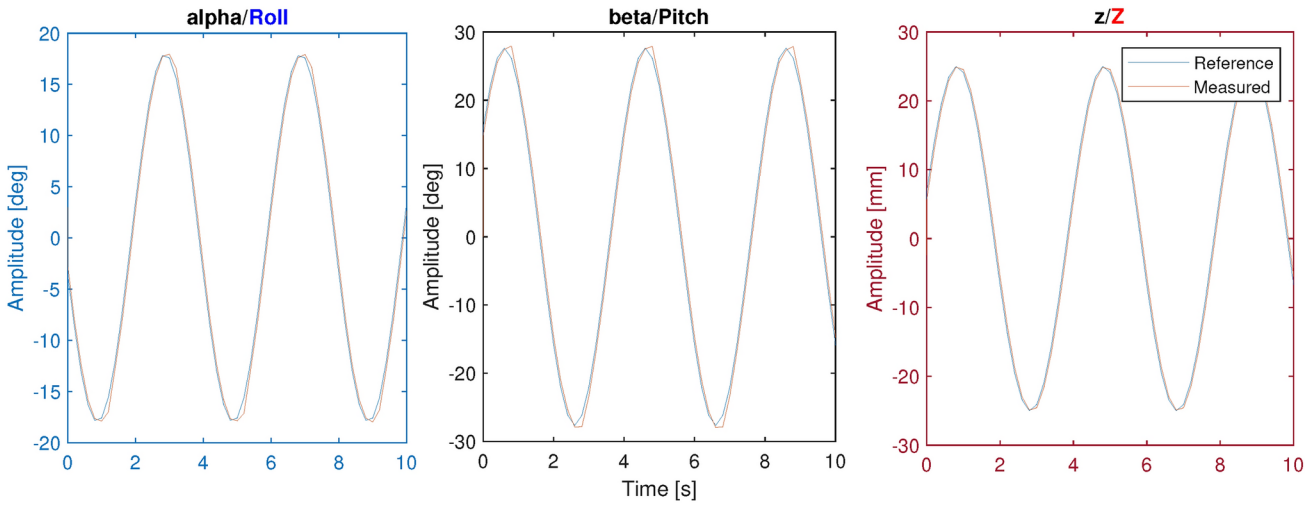

Fig. 17 The evaluation of end effector configuration in alpha during roll rotation, beta angle tracking during pitch rotation, and z position tracking in z translation, respectively

show the movement in the z-translation. Load cell numbers are divided according to the 4 sections on the footplate (see Fig. 1i) starting from the left foot, i.e., the foot sections of the left foot are numbered from 1 to 4 and the right foot sections are numbered from 5 to 8. The distribution in the load cell weight reading is similar to the pressure transfer on the sole of the foot reported in the literature. As seen in the Table 4, approximately 50% of the weight goes to the sole, while the remaining 50% is distributed to the toes and metatarsals [43]. The mean and standard deviation of each load cell showed approximately the same oscillations across each experimental trial. The multiple-trial sets proved the consistency and reliability of the device's performance across different reference inputs.

5 Discussion

Individuals with neurological disorders encounter difficulties in walking, moving, balance, motor control, fatigue, and other health issues, all of which have a major influence on their ADL due to affected CNS and PNS. The PBT program is formed on motor learning principles such as the sequence of training, sensory feedback, assistance, instruction, and focus of attention, as well as exercise physiology principles, e.g., overload, adaptation, progression, individualization, and specificity. This training aims to improve the patient's reaction time, CoM deviation, pressure distribution, APAs and CPAs, thus improving the quality of ADL [13].

Various systems and experimental procedures are developed for different types of disease and severity level. However, since these address specific severity levels, they cannot be used in the entire rehabilitation process. Ankle robots have been produced for patients who cannot stand and move their ankles. Similarly, robotic manipulators for balance rehabilitation are used to improve postural adjustments and reduce the fall rate for patients who can partially support their balance. Another method used to provide improvement in the development of postural adjustments is CSRT. Here, it is aimed that patients who have the capacity to take a step will take steps to certain target points according to the external signal given to analyze postural adjustment parameters. Despite the benefits of robotic therapy, these target points are adjusted manually and do not have sensors to measure GRF. These can be addressed by placing a VF sensor on the end effector of the device and the targeted muscle group during PBT. Moreover, only VR game is used as feedback on these devices/tests thus, they cannot improve re-weighting skills between different senses. This holds significance because, in everyday situations, individuals encounter various stimuli simultaneously.

The proposed BalanSENS system encourages the active participation paradigm from the CNS to the PNS by integrating the aforementioned multi-sensory information with the co-improvement of sensory and motor functions. In order to meet the requirements specified in the I-BaR method, three main segments are integrated into the system. The BalanSENS platform that incorporates I-BaR methodology offers a protocol for individuals with different disease levels to participate in the rehabilitation process. It is explained in three phases, namely, ankle-foot, balance, and stepping. The first phase is for ankle-foot, as patients with severe conditions cannot stand and their ankle muscles are weak, which aims to increase mobility, joint proprioception, and sole sensation. Once the patient's ankle condition improves, rehabilitation procedure continues with the initiation of the balance phase. This phase aims to enhance sensory weighting abilities and provides gradual independence via PBT. The stepping phase aims to improve walking initiation and other walking characteristics by stepping at different target points with distance and direction modulation.

The proposed 3 DoF platform is evaluated in simulation before building the prototype of the system. The system is simulated to select the properties of the servo motors, and analyze the load-bearing capacity and feasibility of the static parts, and the interaction of the selected materials and the servo motors affect the system control with the CTC method. The maximum required force values of the motors are found as 1350 N (see Fig. 5), and then linear actuator characteristics are determined accordingly. Furthermore, the results of feasibility analysis indicate that selected materials do not show significant deformation and are able to carry human weight. Lastly, in the CTC simulation, the maximum RMSE is found to be $3.006\text{x}_{10^{-6}}$ in the first servo motor in Z-transformation. This simulation is conducted to prove that the selected material and linear actuator can be controlled together, and non-linearity due to the parallel manipulator structure can be compensated with CTC.

Following that, the 3 DoF platform is built based on these simulation results. This study investigates the communication and performance characteristics of the servo motors' and load cell sensors to improve overall system performance and capabilities during further prototype construction and rehabilitation testing. Two panels are created to enable the system to communicate, namely a load cell panel and an electrical panel. The reason for the separate panels is to keep load cells' analog signal as long distances as possible so that the analog signal is not affected by 50 Hz power line noise. One of the design testing aims was to analyze the communication of these two panels.

The characteristics of the servo motors and the design of the system are evaluated to see the 3 DoF parallel manipulator and panels' behavior during the ankle preparation phase. In the context of the characterization, a chirp signal (initial frequency starting at 10 Hz and ending at 1 kHz for 120 s) is given as a reference input to the assembled platform, and the output signal is recorded across various frequencies. The crucial facet of the analysis involves the identification of the cut-off frequencies. This frequency indicates a decline in the motor's capacity to precisely and consistently react to input signals. It is vital to stay within the frequency range because, in human-subject experiments, the system must be stable. As the system operates with all motors within a unified control loop, the cut-off frequency for the entire setup is dictated by the lowest frequency among the motors, which was determined to be 6300 Hz (see Fig. 14). The end effector is not symmetrical, so during characterization, a higher force is applied to the first motor which is why its cut-off frequency was found to be lower. This cutoff frequency holds significant importance not only in terms of stability

but also in determining the velocity of perturbation. Considering the I-BaR velocities limitation, the results derived from the characterization tests are found to be satisfactory.

The second servo motor characteristics test was testing the motors on different positions (10–100 mm) and velocities (10–100 mm/s) with accuracy, rise and settling time. The maximum RMSE values are obtained as 0.773 mm when servos are given 100 mm position and 100 mm/s velocity at first servo motors. This position error results in a maximum error of 0.24 degrees in the orientation of the end effector. Although this angle value does not make a significant difference for healthy people, it may be an important value in patients with high spasticity. While this characteristics test provides valuable insights into the performance of the motors, it also revealed certain limitations that should be acknowledged during ankle preparation rehabilitation. This error is due to the non-linear kinematic equations and mechanical imperfections. Such problems are tackled by utilizing CTC to alleviate non-linearity and replacing the ABS material used for the joints with aluminum, respectively. Moreover, the experiment identifies that the maximum rise and settling times occurred when the motors are operated at a position of 100 mm and a relatively lower velocity of 10 mm/s. Additionally, the observed higher torque requirements time during this motion can cause mechanical stress on the system, which could impact its overall longevity and reliability.

The design functionality of the system is tested with one healthy subject with five experimental trials with a three minutes duration and 2 ms sampling rate. As seen in Table 4, approximately 50% of the weight distribution went to the sole, while the remaining 50% is distributed to the toes and metatarsals as stated in literature. Furthermore, as seen in Fig. 16 at each trial, load cell's measurements exhibit approximately the same oscillations across each experimental trial. This consistency in the oscillation patterns demonstrates the system's ability to consistently and accurately capture the applied forces during the exercises since they are conducted with the same healthy subject. It confirms that the system's sensors can provide reliable and consistent data and make it a reliable tool for monitoring and assessing the force exerted during rehabilitation exercises. However, it is important to acknowledge some limitations that arise during this test. First of all, the evaluation is conducted with only one healthy subject. While this provides initial testing feedback, it may not fully represent the wide range of potential users; thus, tests will be conducted with a larger population in the future. Despite these limitations, the functionality tests demonstrate promising results, indicating that the system has the potential to be a valuable tool in the rehabilitation process for force measurement.

Table 5 Mean and standard deviation position tracking RMSE during functionality evaluation experimental trials

Servo motor number	Z-translation [mm]	Roll [mm]	Pitch [mm]
Servo 1	0.699 ± 0.201	4.743e-5 ± 6.981e-6	0.261 ± 5.124e-4
Servo 2	0.699 ± 0.199	0.200 ± 7.095e-4	0.261 ± 5.124e-4
Servo 3	0.695 ± 0.176	0.196 ± 4.879e-4	0.695 ± 5.124e-4

Furthermore, the position tracking of each servo motor on design testing is presented in Table 5. The maximum mean RMSE of position tracking is 0.699 mm at z translation. These position errors result in 0.24 degrees of error in the orientation of the end effector. When the corresponding distances are analyzed, these values are higher than the Simscape CTC simulation. The error arises from mechanical imperfections, such as joint friction and sampling intervals (simulation involves continuity, whereas real-time operation involves signal discretization). Moreover, mechanical imperfections and the non-linearity in kinematic and dynamic equations also contribute to this variation. Consequently, our future aim also involves the application of diverse control techniques aimed at mitigating tracking discrepancies.

Overall, the impact of these characteristics and design tests is evident in the system's ability to track movements and collect data successfully during the ankle preparation phase. The results provide valuable insights into the designed system's performance, serving as a foundation for further refinement and improvement of the system's design. In addition, in this article, the system design was tested on ankle preparation, in other words, the load cell evaluation was made while the system was active and the user was passive (I-BaR framework first testing (Patient Mode: Passive, Device Mode: Active, Feedback: None, and ROM: Max)). In future studies, different control methods will be tested on the servo motor in which patients can actively participate for further I-BaR framework testing (impedance control and CTC, etc.). In addition, patients to be included in the study should be able to stand for at least 60 s and walk at least 10 m without manual assistance. Furthermore, their Functional Ambulation Scale (FAS)<4, Berg Balance Scale (BBS)<40, and Modified Ashworth Scale (MAS)<3 levels should be in the specified range. Thus, the system will be improved to be compatible with the above-mentioned patient group. Moreover, the remaining parts of the system will be prototyped, and balance and stepping rehabilitation will be studied.

6 Conclusion

BalanSENS is designed to adopt an approach that encourages active participation by combining various sensory inputs to enhance both sensory and motor functions. Its ability to customize balance rehabilitation for each individual is achieved within three phases. The initial phase focuses on activating foot-ankle muscles, improving joint mobility, and developing sensation of movement while the individual is in a seated position. In the second phase, the system utilizes multi-sensory inputs during PBT, thereby improving sensory weighting skills and balance. In the final stepping phase, walking parameters are improved by comprehending the correlation between step speed and accuracy.

The system design is appraised by the simulations to detect the required specifications for the servo motors and evaluate the load-bearing capacity, feasibility, and the CTC method. Simulation tests revealed critical performance metrics, including a maximum required force of 1350 N for the servo motors, ensuring that the system can handle the necessary loads during rehabilitation exercises. The simulation also showed that the maximum RMSE is $3.006x10^{-6}$ in the CTC simulation, indicating a high level of accuracy in system control and response. The physical 3 DoF platform is implemented in light of simulation outcomes to facilitate communication between servo motors and sensors. The servo motor characteristics are evaluated through the application of chirp signals, revealing their adequacy for the envisioned application. Moreover, the examinations involving a healthy volunteer carried out to prove the system design functionality exhibited encouraging outcomes in force measurement and real-time data monitoring during rehabilitation routines, despite some constraints. The findings of this study provide a groundwork for our subsequent improvements. In experimental tests conducted with a healthy subject, the system exhibited a maximum RMSE of 0.773 mm for position tracking. This positional error translated into a 0.24-degree deviation in the orientation of the end effector. While this angular discrepancy is relatively minor and may not significantly impact healthy individuals, it is crucial to address in the context of patients with high spasticity or other motor control issues, as even small errors can have more pronounced effects on their rehabilitation outcomes. These results underscore the system's potential for precise movement tracking and force measurement while also highlighting areas for refinement to enhance accuracy and performance further. While the experiments verified the reliability of the device, future studies will include stroke patients with mild-to-moderate motor impairments in the affected ankle with foot gait abnormality in the ankle phase. After the ankle phase, the balance phase will be started, and trunk sway, CoM deviation, reaction time, and force distribution in the haptic bar will be evaluated in the patients. Final rehabilitation tests include the stepping phase and the reaction time and weight transfer capacity will be evaluated.

Author Contributions TE and PK were responsible for the literature survey of the whole system. PK, EH, and RU supervised the study. All authors contributed to the manuscript revision, read, and approved the submitted version.

Funding This research is supported by The Scientific and Technological Research Council of Türkiye (TUBITAK) under Grant 122E246. The funders had no role in study design, data collection and analysis, decision to publish, or preparation of the manuscript.

Availability of Data and Materials Data are available.

Code Availability Not applicable.

Declarations

Conflict of Interest The authors declare that they have no conflict of interest.

Ethical Approval and Research Involving Human and Animal Participants The studies involving human participants are reviewed and approved by the University Research Ethics Council of Istanbul Medipol University under the E-66291034-772.02-4494 number.

Consent to Participate The participant provided their written informed consent to participate in this study.

Consent for Publication The participant provided their written informed consent to publish the data in this study.

References

1. WHO (2022, 19 May). *World health statistics 2022: monitoring health for the SDGs, sustainable development goals*. Retrieved: Jul. 03, 2022 from: https://www.who.int/publications/i/item/9789240051157.
2. Horak, F. B. (2006). Postural orientation and equilibrium: What do we need to know about neural control of balance to prevent falls? *Age and Ageing,35*, 7–11.
3. Craig, J. J., Bruetsch, A. P., Lynch, S. G., & Huisinga, J. M. (2019). Altered visual and somatosensory feedback affects gait stability in persons with multiple sclerosis. *Human Movement Science,66*, 355–362.
4. Aruin, A. (2016). Enhancing anticipatory postural adjustments: A novel approach to balance rehabilitation. *Journal of Novel Physiotherapies,6*, 10–12.
5. Aruin, A. S., Ganesan, M., & Lee, Y. (2017). Improvement of postural control in individuals with multiple sclerosis after a single-session of ball throwing exercise. *Multiple sclerosis and related disorders,17*, 224–229.
6. Ersoy, T., Kaya, P., Hocaoglu, E., & Unal, R. (2024). I-bar: integrated balance rehabilitation framework. *Frontiers in Neurorobotics,18*, 1401931.
7. Tajali, S., Rouhani, M., Mehravar, M., Eteraf-Oskouei, A., Negahban, H., & Sadati, E. (2017). Effects of external perturbations on

anticipatory and compensatory postural adjustments in patients with multiple sclerosis who have a previous fall history. *International Journal of MS Care,20*, 164.
8. Krishnan, V., Kanekar, N., & Aruin, A. S. (2012). Anticipatory postural adjustments in individuals with multiple sclerosis. *Neuroscience Letters,506*, 256–260. https://doi.org/10.1016/j.neulet.2011.11.018
9. Shadmehr, A., & Amiri, S. (2012). Design and construction of a computerized based system for reaction time test and anticipation skill estimation. *International Journal of Bioscience, Biochemistry and Bioinformatics,2*, 429–432.
10. Aruin, A. S., Kanekar, N., Lee, Y. J., & Ganesan, M. (2015). Enhancement of anticipatory postural adjustments in older adults as a result of a single session of ball throwing exercise. *Experimental Brain Research,233*, 649–655.
11. Yamada, H., & Shinya, M. (2021). Variability in the center of mass state during initiation of accurate forward step aimed at targets of different sizes. *Frontiers in Sports and Active Living,3*, 691307.
12. Aruin, A. S., Ganesan, M., & Lee, Y. (2017). Improvement of postural control in individuals with multiple sclerosis after a single-session of ball throwing exercise. *Multiple Sclerosis and Related Disorders,17*, 224–229.
13. Mansfield, A., Aqui, A., Centen, A., Danells, C. J., DePaul, V. G., Knorr, S., Schinkel-Ivy, A., Brooks, D., Inness, E. L., & McIlroy, W. E. (2015). Perturbation training to promote safe independent mobility post-stroke: Study protocol for a randomized controlled trial. *BMC Neurology,15*, 1–10.
14. Pai, Y. C., Yang, F., Bhatt, T., & Wang, E. (2014). Learning from laboratory-induced falling: long-term motor retention among older adults. *Age (Dordrecht, Netherlands),36*, 1367–1376.
15. Bhatt, T., & Pai, Y. C. (2008). Immediate and latent interlimb transfer of gait stability adaptation following repeated exposure to slips. *Journal of Motor Behavior,40*, 380–390.
16. Bhatt, T., & Pai, Y. C. (2009). Generalization of gait adaptation for fall prevention: from moveable platform to slippery floor. *Journal of Neurophysiology,101*, 948–957.
17. Gerards, M. H. G., McCrum, C., Mansfield, A., & Meijer, K. (2017). Perturbation-based balance training for falls reduction among older adults: Current evidence and implications for clinical practice. *Geriatrics Gerontology International,17*, 2294–2303.
18. Pai, Y. C., & Bhatt, T. S. (2007). Repeated-slip training: An emerging paradigm for prevention of slip-related falls among older adults. *Physical Therapy,87*, 1478.
19. Mansfield, A., Inness, E. L., Komar, J., Biasin, L., Brunton, K., Lakhani, B., & Mcilroy, W. E. (2011). Training rapid stepping responses in an individual with stroke. *Physical therapy,91*, 958–969.
20. Aviles, J., Wright, D. L., Allin, L. J., Alexander, N. B., & Madigan, M. L. (2020). Improvement in trunk kinematics after treadmill-based reactive balance training among older adults is strongly associated with trunk kinematics before training. *Journal of Biomechanics,113*, 110112.
21. Tanvi, B., Feng, Y., & Yi-Chung, P. (2012). Learning to resist gait-slip falls: long-term retention in community-dwelling older adults. *Archives of Physical Medicine and Rehabilitation,93*, 557–564.
22. Prosperini, L., & Pozzilli, C. (2013). The clinical relevance of force platform measures in multiple sclerosis: A review. *Multiple Sclerosis International,2013*, 1–9.
23. Huno (2021). *Huno, robotic rehabilitation system*. Retrieved: Aug. 17, 2021 from: https://www.movendo.technology/our-products/huno/?lang=en.
24. Bobo-Balance (2021). *Bobo Smart Physical Therapy Tools*. Retrieved: Aug. 17, 2021, from: https://bobo-balance.com/.
25. Vertigomed-Prodotti (2021). *Vertigomed Prodotti*. Retrieved: Aug. 17, 2021, from: http://vertigomed.it/uk/index.php/vertigomed-prodotti/geapro/.
26. Huber (2022). *Huber 360: Evolution push the boundaries with the new Huber evolution*. Retrieved: Jul. 03, 2022 from: https://www.lpgmedical.com/en/professional-area/huber/.
27. Tiseo, C., Lim, Z. Y., Shee, C. Y. & Ang, W. T., Mobile robotic assistive balance trainer-an intelligent compliant and adaptive robotic balance assistant for daily living, IEEE engineering in medicine and biology society (2014), 5300–5303.
28. Sinitski, E. H., Lemaire, E. D., & Baddour, N. (2015). Evaluation of motion platform embedded with force plate-instrumented treadmill. *Journal of Rehabilitation Research & Development,52*, 221–233.
29. El Makssoud, H., Richards, C. L. & Comeau, F., Dynamic control of a moving platform using the caren system to optimize walking invirtual reality environments, International Conference of the IEEE Engineering in Medicine and Biology Society (2009), 2384–2387.
30. Girone, M., Burdea, G., Bouzit, M., Popescu, V., & Deutsch, J. E. (2001). A stewart platform-based system for ankle telerehabilitation. *Autonomous Robots,10*, 203–212.
31. Saglia, J. A., Tsagarakis, N. G., Dai, J. S., & Caldwell, D. G. (2013). Control strategies for patient-assisted training using the ankle rehabilitation robot (arbot). *IEEE/ASME Transactions on Mechatronics,18*, 1799–1808.
32. Li, J., Zhou, Y., Dong, M., Rong, X., & Jiao, R. (2023). Clinically oriented ankle rehabilitation robot with a novel $R-2Ups/rr$ mechanism. *Robotica,41*, 277–291.
33. Teramae, T., Noda, T., & Morimoto, J. (2018). Emg-based model predictive control for physical human-robot interaction: Application for assist-as-needed control. *IEEE Robotics and Automation Letters,3*, 210–217.
34. Keller, U., Rauter, G., & Riener, R. (2013). Assist-as-needed path control for the pascal rehabilitation robot. *IEEE International Conference on Rehabilitation Robotics,2013*, 1–7.
35. Luo, L., Peng, L., Wang, C., & Hou, Z. G. (2019). A greedy assist-as-needed controller for upper limb rehabilitation. *IEEE Transactions on Neural Networks and Learning Systems,30*, 3433–3443.
36. Mazare, M., Tolu, S., & Taghizadeh, M. (2021). Adaptive variable impedance control for a modular soft robot manipulator in configuration space. *Meccanica,57*, 1–15.
37. Morone, G., Ghanbari Ghooshchy, S., Palomba, A., Baricich, A., Santamato, A., Ciritella, C., Ciancarelli, I., Molteni, F., Gimigliano, F., & Iolascon, G. (2021). Differentiation among bio- and augmented- feedback in technologically assisted rehabilitation. *Expert Review of Medical Devices,18*, 513–522.
38. Barr, C., McLoughlin, J., Lord, S. R., Crotty, M., & Sturnieks, D. L. (2014). Walking for six minutes increases both simple reaction time and stepping reaction time in moderately disabled people with multiple sclerosis. *Multiple Sclerosis and Related Disorders,3*, 457–462.
39. Bourrelier, J., Fautrelle, L., Haratyk, E., Manckoundia, P., Mérienne, F., Mourey, F., & Kubicki, A. (2021). Enhancement of anticipatory postural adjustments by virtual reality in older adults with cognitive and motor deficits: A randomised trial. *Geriatrics,6*, 72.
40. Gide, A. (1967). *Anthropometry*. Angewandte Chemie International Edition: Ergonomics and the Design of Work.
41. Ersoy, T., & Hocaoglu, E. (2023). A 3-dof robotic platform for the rehabilitation and assessment of reaction time and balance skills of ms patients. *PLOS ONE,18*, 1–36. https://doi.org/10.1371/journal.pone.0280505
42. Hasan, S. K., & Dhingra, A. K. (2020). State of the art technologies for exoskeleton human lower extremity rehabilitation robots. *Journal of Mechatronics and Robotics,4*, 211–235.

43. Perttunen, J. (2002). *Foot loading in normal and pathological walking* 83. University of Jyväskylä.
44. Chien, J. H., Ambati, V. N. P., Huang, C. K., & Mukherjee, M. (2017). Tactile stimuli affect long-range correlations of stride interval and stride length differently during walking. *Experimental Brain Research,235*, 1185–1193.
45. De Angelis, S., Princi, A. A., Dal Farra, F., Morone, G., Caltagirone, C., & Tramontano, M. (2021). Vibrotactile-based rehabilitation on balance and gait in patients with neurological diseases: A systematic review and metanalysis. *Brain Sciences,11*, 518.